

Influence of Fluoride Substitution on the Physicochemical Properties of LiMn_2O_4 Cathode Materials for Lithium-ion Batteries

PaulosTadesseShibeshi, V. Veeraiah, A.V. PrasadaRao

Abstract— $\text{LiMn}_2\text{O}_{4-x}\text{F}_x$ ($x = 0.00, 0.04$ and 0.1) cathode materials were synthesized from Li_2CO_3 , MnO_2 and LiF precursors by solid-state reaction method at 800°C in air. The influence of fluoride substitution on the physicochemical properties of LiMn_2O_4 cathode has been investigated by different techniques. From the Thermogravimetric and Differential Thermogravimetric (TG/DTG) curves, it is clearly observed that substitution of fluorine attributed to the faster fabrication of $\text{LiMn}_2\text{O}_{3.96}\text{F}_{0.04}$ and $\text{LiMn}_2\text{O}_{3.9}\text{F}_{0.1}$ cathode materials. By Powder X-ray Diffraction (XRD) analysis, the synthesized materials are detected as single phase spinel structure having a space group $\text{Fd}3\text{m}$. However, the diffraction peaks shifted to lower angles and the lattice parameter increases with substitution of fluorine. Redox titration tests confirmed that the average oxidation state of manganese in fluoride substituted samples is lower than that of pure one (LiMn_2O_4). Scanning Electron Microscopy (SEM) investigations demonstrated that substitution of fluorine reduced the agglomeration of powder particles. Also, fluorine substituted samples have greater grain size than the pure one (LiMn_2O_4). Further, the Energy Dispersive Spectroscopy (EDS) analysis confirmed the incorporation of fluorine in to $\text{LiMn}_2\text{O}_{3.96}\text{F}_{0.04}$ and $\text{LiMn}_2\text{O}_{3.9}\text{F}_{0.1}$ spinel samples. Strong frequency bands, responsible for the formation of all samples, are observed from Fourier Transform Infrared (FT-IR) Spectroscopy spectra. However, the bands for fluoride substituted samples are shifted slightly towards lower wave numbers.

Index Terms—cathode materials, Lithium- ion battery, solid state-reaction, substitution of fluorine

1 INTRODUCTION

Lithium-ion batteries are the fundamental power sources for portable electronic devices such as digital camera, video camera (camcorder), laptops, personal digital assistants (PDA), cellular phone and the like. They are also attractive for high power applications such as electric vehicles and hybrid electric vehicles due to their long cycle life and high energy density [1,2-5]. The most widely used commercial cathode material for lithium-ion batteries is

LiCoO_2 due to its easy synthesis, stable electrochemical cycling, high reversibility and long cycle life. However, this material has some drawbacks: toxic (high impact to the environment) [5-7], expensive due to limited sources of Co [5,6], structural deformation when more than 0.5 lithium ions are removed from it, and inherent safety problem [1,7].

In this regard, there is a strong interest worldwide in developing alternative low cost, high electrical potential and non-toxic cathode materials [8] for application of lithium-ion batteries. Among the promising candidates, spinel LiMn_2O_4 is an attractive cathode material that shows much attention due to its lower cost, low toxicity, high voltage source, and good safety compared with the LiCoO_2 [9,10]. However, LiMn_2O_4 suffers severe capacity fade on cycling particularly at elevated temperature (above 40°C) at which most electronic devices operate [9-11]. This capacity fade is associated with the dissolution of manganese into electrolyte [11], Jahn-Teller distortion of Mn^{3+} ions [10,11], decomposition of electrolyte solution on the electrode [12], and formation of lattice parameter difference between two cubic phases formed during charge-discharge process [1,10,11].

-
- PaulosTadesseShibeshi is presently a research scholar in the Department of Physics, College of Science and Technology, Andhra University, Visakhapatnam-530 003, INDIA. E-mail: Kidspaul@gmail.com.
 - V. Veeraiah is a professor in the Department of Physics and Principal of Science and Technology College, Andhra University, Visakhapatnam-530 003, INDIA.
 - A.V. PrasadaRao is a professor in the Department of Inorganic & Analytical Chemistry, College of Science and Technology, Andhra University, Visakhapatnam-530 003, INDIA

In order to improve the performance of LiMn_2O_4 related with surface morphology, many research works have been carried out which include directly preparing spinel with small surface area, and also by surface coating (surface modifications) such as MgO , Al_2O_3 , SiO_2 and TiO_2 [13-15]. Also, many efforts have been devoted to enhance the structural stability and other electrochemical properties. Among these, partial substitution of cations such as Co^{3+} , Ni^{2+} , Fe^{2+} , Cr^{3+} , Al^{3+} , Mg^{2+} , Ga^{3+} into Mn sites is widely reported [1,9,14]. However, the cationic replacement into the spinel lattice has the effect of decreasing the initial reversible capacity [16], which may make this type of spinel unattractive for practical application. Also, the above methods could not totally overcome the capacity fade problem. In order to improve the reversible capacity of the spinel LiMn_2O_4 , nowadays partial substitution of anion such as F^- , Cl^- , S^{2-} , Br^- for O^{2-} has been reported. For instance, Chen Zhao-yong et al [17] demonstrated that the substitution of F^- , Cl^- and Br^- for O^{2-} leads to an increase of the reversible capacity.

LiMn_2O_4 has a spinel structure of space group $\text{Fd}\bar{3}\text{m}$ and contains 3 types of cations: Li^+ , Mn^{3+} and Mn^{4+} , and one type of anion O^{2-} . The structure consists cubic close-packed oxygen ions in 32e sites, lithium ions in the 8a tetrahedral sites, and manganese ions (Mn^{3+} and Mn^{4+}) in the 16d octahedral sites [11,18]. This structure provides a three dimensional network of face-sharing tetrahedra and octahedra for lithium ion diffusion.

In this study, we report the synthesis of LiMn_2O_4 , $\text{LiMn}_2\text{O}_{3.96}\text{F}_{0.04}$ and $\text{LiMn}_2\text{O}_{3.9}\text{F}_{0.1}$ cathode materials by one step solid-state reaction method. Effect of synthesis conditions and influence of substitution of F^- for O^{2-} on the physicochemical properties of the powder materials have been examined systematically by using Thermogravimetric and Differential Thermogravimetric (TG/DTG), powder X-ray Diffraction (XRD), Scanning Electron Microscopy (SEM), Energy Dispersive Spectroscopy (EDS), redox-titration method with oxalate, and Fourier Transform Infrared (FT-IR) spectroscopy.

2 EXPERIMENT

$\text{LiMn}_2\text{O}_{4-x}\text{F}_x$ ($x = 0.00, 0.04$ and 0.1) samples were synthesized in the form of powder by conventional solid-state reaction with precursors Li_2CO_3 (99%, Merck), MnO_2 (99%, Himedia) and LiF (99.5%, Himedia). A mixture of stoichiometric Li_2CO_3 (3% excess) and MnO_2 was ground

in agate mortar for synthesis of LiMn_2O_4 . Similarly, stoichiometric raw materials Li_2CO_3 (2% excess), MnO_2 and LiF (1% excess) were mixed and ground in agate mortar for synthesis of fluoride substituted samples ($\text{LiMn}_2\text{O}_{3.96}\text{F}_{0.04}$ and $\text{LiMn}_2\text{O}_{3.9}\text{F}_{0.1}$). After through homogenizing, the powders were heated and subjected to heat treatment at 800°C for 24 hrs in air, followed by slow cooling rate of $1^\circ\text{C}/\text{min}$. A slight excess amount of lithium and fluorine was used to compensate for losses of lithium and fluorine during calcination process.

TG/DTG measurements were conducted using Mettler Toledo instrument from room temperature to 850°C in oxygen atmosphere at a heating rate of $10^\circ\text{C}/\text{min}$ to find out the temperature at which crystallization of the sample is completed.

Phase identification was carried out by XRD using a Phillips XPERT-PRO diffractometer fitted with $\text{Cu } K_\alpha$ radiation ($\lambda = 1.54060 \text{ \AA}$) between $2\theta = 10^\circ$ and 90° in steps of 0.017° (2θ) with a constant counting time of 24.765 s. The unit cell lattice parameters were obtained by the least square fitting method from the d-spacing and the hkl values.

SEM measurements were performed using JSM-6610 instrument to examine the morphology of the calcined powders. EDS, coupled with SEM, studies were conducted to investigate the incorporation of fluorine in to fluoride substituted synthesized active materials.

The average oxidation state of manganese was determined by redox-titration method with oxalate. About 50 mg of each spinel sample was dissolved in 20 ml of an acidified 0.05N $\text{Na}_2\text{C}_2\text{O}_4$ solution in 20 ml of 4N H_2SO_4 . Further, the remaining unreacting oxalate was back titrated with 0.05N KMnO_4 solution.

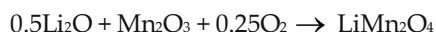
FT-IR spectra were recorded using ALFA-T spectrometer with the KBr pellet method in the wave number region of from $400\text{--}4,000 \text{ cm}^{-1}$.

3 RESULT AND DISCUSSION

3.1 Thermal Analysis

Figure 1 shows the TG and DTG curves for LiMn_2O_4 , $\text{LiMn}_2\text{O}_{3.96}\text{F}_{0.04}$ and $\text{LiMn}_2\text{O}_{3.9}\text{F}_{0.1}$ powders heated at $10^\circ\text{C}/\text{min}$ in flowing oxygen. As seen from all curves, there is an initial weight loss in the temperature range from room temperature to 250°C , corresponding to the evaporation of methanol alcohol added in order to homogenize the mixture during grinding and the moisture absorbed during storage. TG curve of LiMn_2O_4 shows significant weight loss (12.71 %)

between temperatures 300 °C and 500 °C. This loss is attributed to the decomposition of the precursors Li_2CO_3 and MnO_2 ; and the reaction between decomposed materials in order to produce crystalline LiMn_2O_4 . This is supported by sharp peak observed at 390 °C on the DTG curve. The decomposition reaction of the precursors and the reaction between decomposed materials process are expressed as:



Li_2CO_3 and MnO_2 are stable in air up to 750 °C [19] and 535 °C [20] respectively. However, in reaction mixture with several oxides they can be decomposed at lower temperature. After 490 °C, a slight weight loss is observed (2.02 %), attributed to more decomposition of remaining precursor materials. It can also be seen from the figure that at higher temperatures, the TG curve becomes more flattened, indicating the stable phase formation. Finally, the total weight loss for over all reaction is 15.26 %, which is slightly larger than the theoretical result of 14.25 %. This difference is happened due to slight excess amount of Li_2CO_3 precursor was used to compensate for losses of lithium during the calcination process.

On the observation over the TG and DTG curves obtained from fluoride substituted precursors, it is indicated that there is a maximum loss between 300 °C and 500 °C. This loss is suggested the decomposition of the precursors Li_2CO_3 and MnO_2 , and the reaction between decomposed materials. This is supported by sharp peak observed at about 387 °C on the DTG curves. On further heating, we obtained another two smaller sharp peaks between 500 °C and 625 °C which were not observed from LiMn_2O_4 curve. It is suggested that the first peaks (fig.1 b and c) at about 561 °C are due to the reaction between decomposed materials in order to produce crystalline $\text{LiMn}_2\text{O}_{3.96}\text{F}_{0.04}$ and $\text{LiMn}_2\text{O}_{3.9}\text{F}_{0.1}$. The next sharp peaks at about 610 °C are corresponding to melting of the undecomposed part of LiF followed by evaporation of fluorine or volatilization of LiF itself. The decomposition reaction of the precursors and the reaction between decomposed materials process are expressed as:

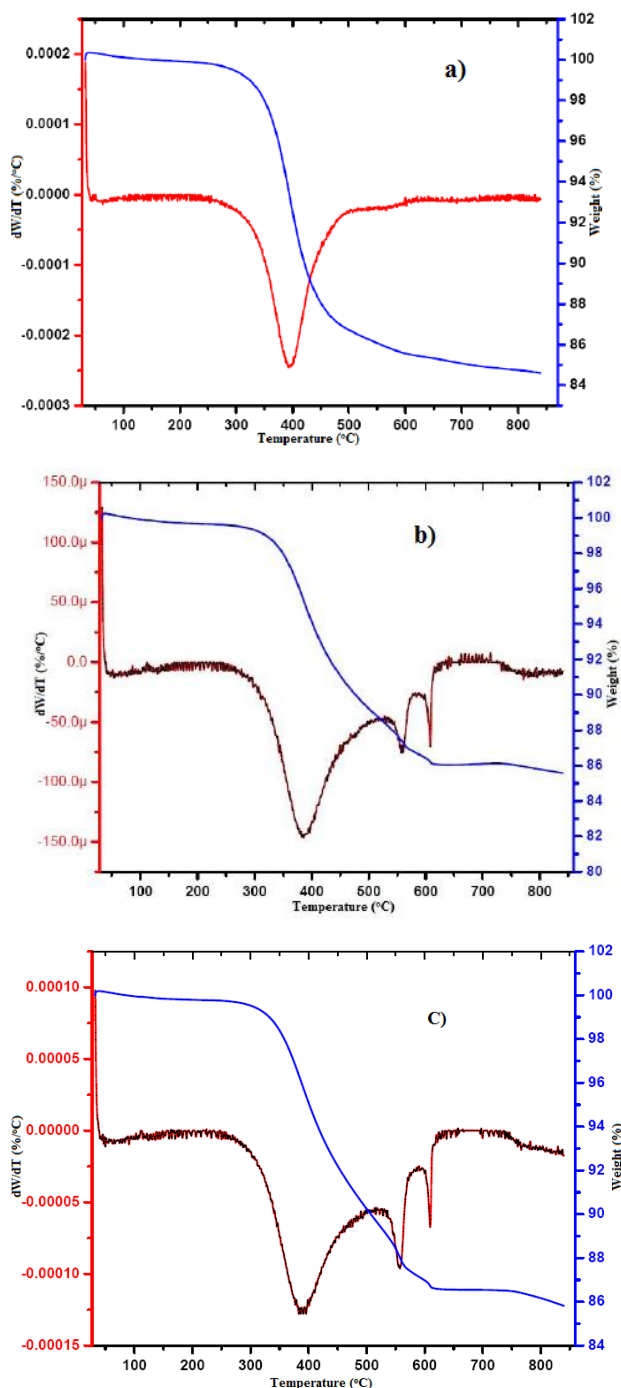
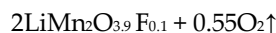
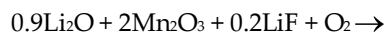
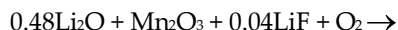


Fig. 1. TG and DTG curves for a) LiMn_2O_4 b) $\text{LiMn}_2\text{O}_{3.96}\text{F}_{0.04}$ and c) $\text{LiMn}_2\text{O}_{3.9}\text{F}_{0.1}$

In comparison with LiMn_2O_4 , the complete crystallization of $\text{LiMn}_2\text{O}_{3.96}\text{F}_{0.04}$ and $\text{LiMn}_2\text{O}_{3.9}\text{F}_{0.1}$ occurs at lower temperature. From this we can deduce that substitution of fluorine attributed to the faster fabrication of the $\text{LiMn}_2\text{O}_{3.96}\text{F}_{0.04}$ and $\text{LiMn}_2\text{O}_{3.9}\text{F}_{0.1}$ powder materials. This faster production of powders is the result of melting of the undecomposed part of the LiF intensifies the reactions.

3.2 XRD Analysis

Figure 2 presents the well defined XRD patterns of powders produced by solid state reaction method heated at 800°C for 24 hours in air. All peaks appeared in the XRD spectrum are very sharp and well-defined, indicating a high crystallinity of the powder materials. Also, no additional impurity peaks are detected. All samples are identified as a single phase of spinel structure with a space group $\text{Fd}\bar{3}\text{m}$, agree well with JCPDS 35-0782 card. Therefore, it is deduced that Li ions occupy tetrahedral 8a sites, Mn ions (Mn^{3+} and Mn^{4+}) occupy octahedral 16d sites, and oxygen and fluorine ions are located at the 32e sites. However, as compared with LiMn_2O_4 , the diffraction lines or 2θ angles of $\text{LiMn}_2\text{O}_{3.96}\text{F}_{0.04}$ and $\text{LiMn}_2\text{O}_{3.9}\text{F}_{0.1}$ materials are shifted slightly towards smaller angles.

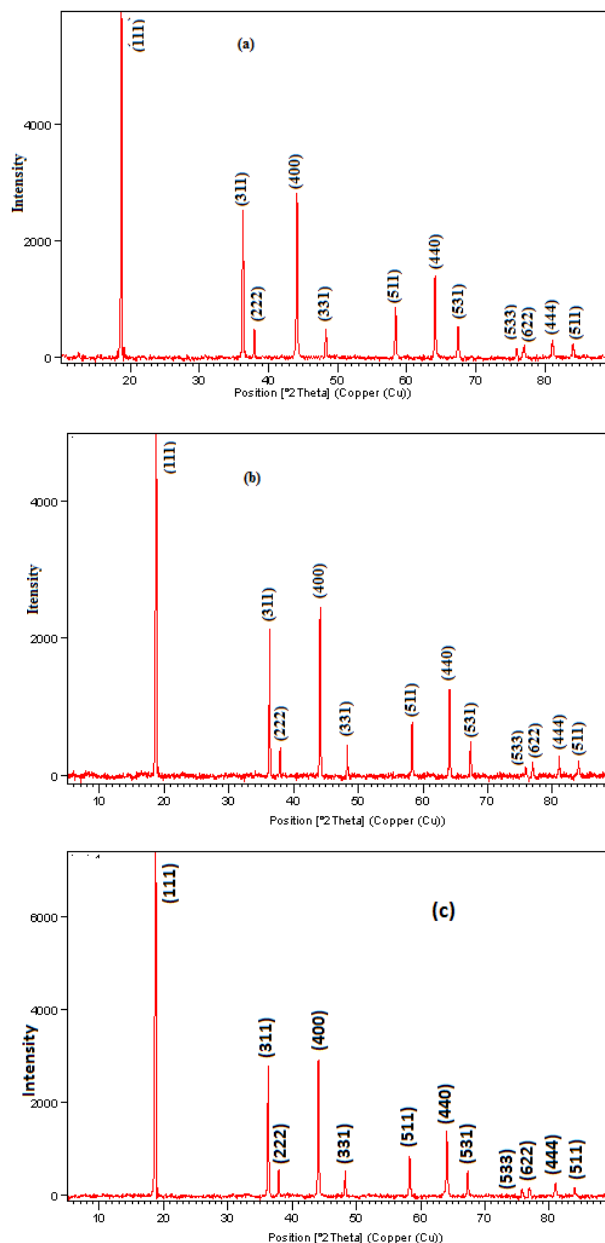
In order to evaluate the influence of partial fluorine substitution on the crystalline lattice of the obtained spinels, we calculated lattice parameters by the least-squares method and cell volume of the samples from XRD data (see table 1). As it can be seen from the table, the lattice parameters of fluoride contained spinels

TABLE 1
LATTICE CONSTANT, CELL VOLUME AND AVERAGE OXIDATION STATE OF Mn OF ALL SAMPLES

Samples	Lattice constant a (Å)	Unit cell Volume (Å) ³	Average oxidation state of Mn
LiMn_2O_4	8.2061	552.60	3.52
$\text{LiMn}_2\text{O}_{3.96}\text{F}_{0.04}$	8.2109	553.57	3.49
$\text{LiMn}_2\text{O}_{3.9}\text{F}_{0.1}$	8.2148	554.36	3.47

slightly increase compared with the pure one (LiMn_2O_4). Also, the lattice constant increases with an increase in the substituted fluorine content, which is related to substitution of fluorine decreases the average Mn valence or it reduces the concentration of the smaller Mn^{4+} ions (ionic radius 0.67Å) into larger Mn^{3+} ions (ionic radius 0.79Å) to maintain charge neutrality in the lattice. This leads to Li-Mn-O bond in LiMn_2O_4 is

stronger than that of Li-Mn-O(F) bond in $\text{LiMn}_2\text{O}_{3.96}\text{F}_{0.04}$ and $\text{LiMn}_2\text{O}_{3.9}\text{F}_{0.1}$, which could enhance the lithium ion movements in the spinels. On the other hand, the variation of lattice parameters of the synthesized spinels and shift of the diffractions lines or 2θ



θ angles

Fig. 2. XRD patterns of a) LiMn_2O_4 b) $\text{LiMn}_2\text{O}_{3.96}\text{F}_{0.04}$ and c) $\text{LiMn}_2\text{O}_{3.9}\text{F}_{0.1}$

towards smaller angles mentioned above reveal the effective replacement of oxygen by fluorine in the lattice.

3.3 Redox Titration Test

Redox titration tests confirmed that (table 1) the average oxidation state of manganese in fluoride substituted samples is lower than that of pure one (LiMn_2O_4). Also, their average oxidation states obtained were slightly less than 3.5. This suggests that substitution of oxygen by fluorine causes the reaction $\text{Mn}^{4+} \rightarrow \text{Mn}^{3+}$, as the result a slight higher Mn^{3+} content and lower Mn^{4+} content appeared in fluorine substituted spinel samples. This is consistent with the observed increase in the lattice constants.

3.4 SEM and EDS Studies

The morphology and grain size of active materials LiMn_2O_4 , $\text{LiMn}_2\text{O}_{3.96}\text{F}_{0.04}$ and $\text{LiMn}_2\text{O}_{3.9}\text{F}_{0.1}$ are shown in figure 3 and table 1 respectively. As seen from the figure, morphological changes are clearly observed as a result of fluorine substitution. This indicates that substitution of fluorine reduced agglomeration of the

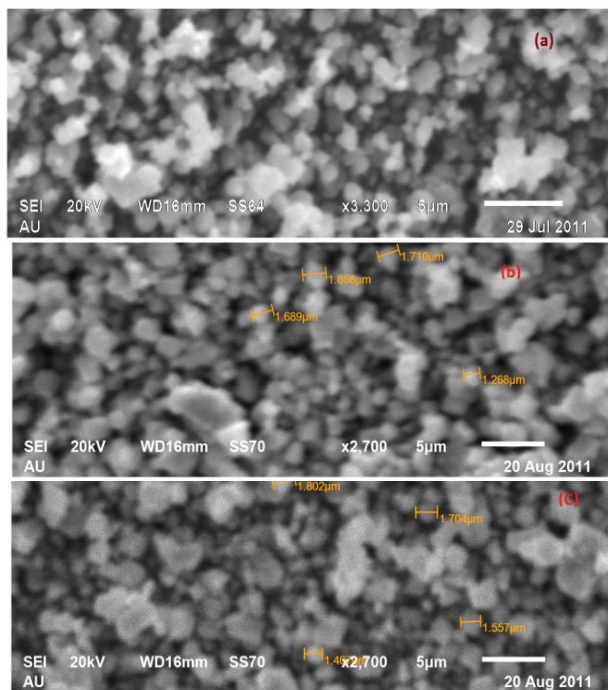


Fig. 3. The SEM Micrograph of a) LiMn_2O_4 b) $\text{LiMn}_2\text{O}_{3.96}\text{F}_{0.04}$ and c) $\text{LiMn}_2\text{O}_{3.9}\text{F}_{0.1}$

powder particles. Such kind of morphology is very important to have good electrochemical properties of the materials. On the other hand, LiMn_2O_4 sample has micro-sized grains of average size about $0.8 \mu\text{m}$, also for $\text{LiMn}_2\text{O}_{3.96}\text{F}_{0.04}$ and $\text{LiMn}_2\text{O}_{3.9}\text{F}_{0.1}$ samples about 1.5

μm and $1.9 \mu\text{m}$, respectively. It is in good agreement with the larger lattice parameter of fluorine contained samples calculated from the XRD patterns. Further, the EDS analysis is carried out to verify the incorporation of fluorine into $\text{LiMn}_2\text{O}_{3.96}\text{F}_{0.04}$ and $\text{LiMn}_2\text{O}_{3.9}\text{F}_{0.1}$ samples. As shown in fig. 4, the presence of fluorine is detected in both samples synthesized by heating with LiF at 800°C for 24 hours.

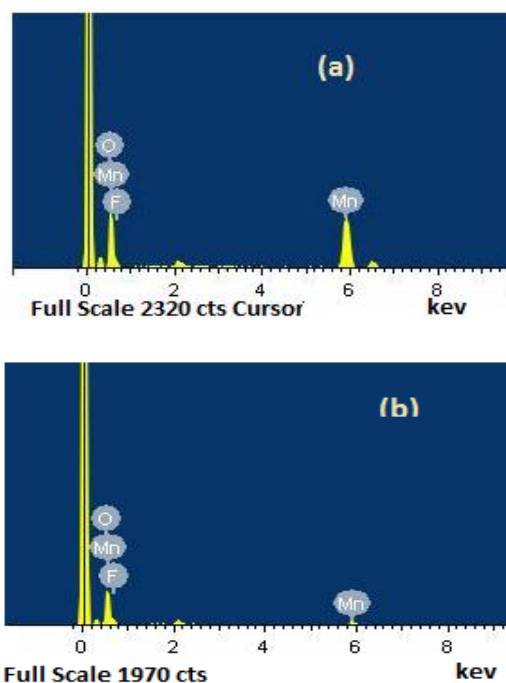


Fig. 4. The EDS spectra of a) $\text{LiMn}_2\text{O}_{3.96}\text{F}_{0.04}$ and b) $\text{LiMn}_2\text{O}_{3.9}\text{F}_{0.1}$

3.5 FT-IR Spectroscopy Study

In order to confirm the results of XRD analysis, the room temperature FT-IR spectra of the synthesized samples are shown in Figure 5. Two distinct peaks are observed in each FT-IR spectrum at different wavelength regions. The two strong frequency bands appeared at wave numbers 623.13 and 521.06 cm^{-1} (fig 5a) are responsible for the formation of LiMn_2O_4 which may be attributed to the asymmetric stretching modes of Li-Mn-O. On the other hand, due to the formation of $\text{LiMn}_2\text{O}_{3.96}\text{F}_{0.04}$ and $\text{LiMn}_2\text{O}_{3.9}\text{F}_{0.1}$ materials, these two peaks are shifted slightly towards lower wave numbers 621.74 and 518.99 cm^{-1} (fig 5b), and 618.99 and 501.33 cm^{-1} (fig.5c), respectively, which may be attributed to the asymmetric stretching modes of Li-Mn-O(F). This is consistent with the assumption deduced from XRD results. Also, it is in good agreement with the larger lattice parameter of fluorine contained samples

calculated from the XRD spectrum. Moreover, the shift of the bands towards lower wave numbers may be pointed out that the replacement of fluorine weakens the strength of Li-Mn-O bonds which is beneficial to enhance the lithium ion movements in the spinels.

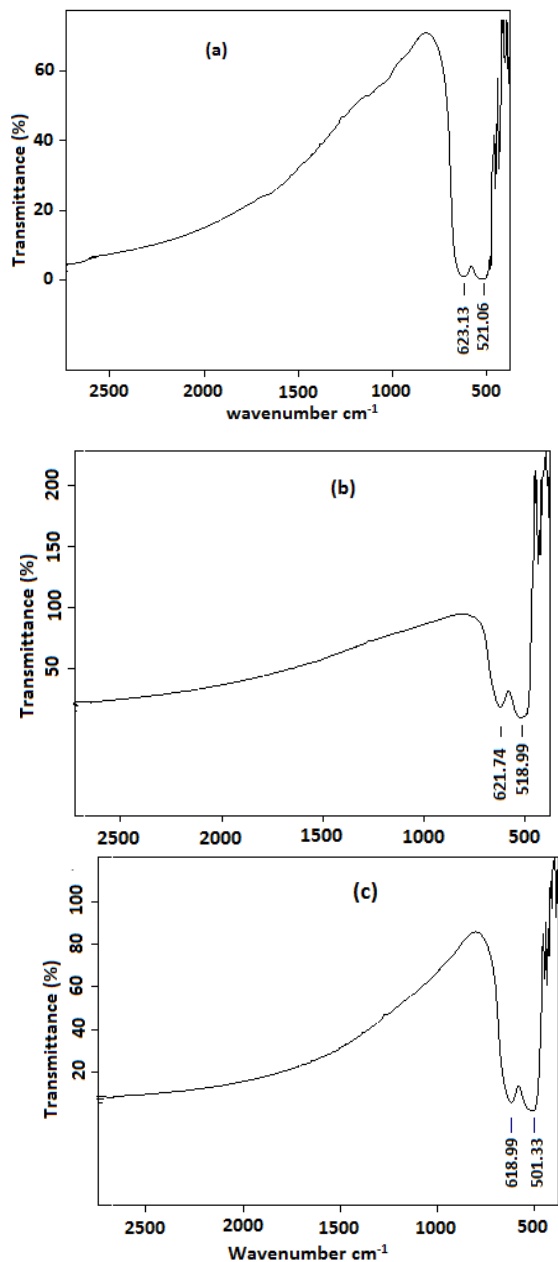


Fig. 5. FT-IR spectra of a) LiMn_2O_4 b) $\text{LiMn}_2\text{O}_{3.96}\text{F}_{0.04}$ and c) $\text{LiMn}_2\text{O}_{3.9}\text{F}_{0.1}$

4 Conclusion

We have attempted to synthesize $\text{LiMn}_2\text{O}_{4-x}\text{F}_x$ ($x = 0, 0.04, \text{ and } 0.1$) powders by the means of one step solid-state reaction method. In this study, their variations in physicochemical properties of the powders were

examined. From the TG/DTG curves, it is clearly observed that substitution of fluorine attributed to the faster fabrication of the spinel $\text{LiMn}_2\text{O}_{3.96}\text{F}_{0.04}$ and $\text{LiMn}_2\text{O}_{3.9}\text{F}_{0.1}$ powder materials. From the structural analysis by XRD, we observed that the synthesized samples showed spinel cubic structure of space group $\text{Fd}\bar{3}\text{m}$, which is well supported by FT-IR spectroscopy study results. Fluorine ion replaced samples exhibit larger lattice parameter with decreasing the average oxidation number of Mn as well as greater grain size than the pure one (LiMn_2O_4). Further, the EDS analysis revealed that fluorine ions are successfully incorporated into the spinel structure of lithium manganese oxide material.

ACKNOWLEDGMENT

The authors would like to thank Prof. N. Someswara Rao for performing TG measurement.

REFERENCES

- [1] Xifei Li, Youlong Xu, "Novel method to enhance the cycling performance of spinel LiMn_2O_4 ", *Electrochemistry Communications*, Vol.9, pp. 2023–2026, 2007.
- [2] Myoung Youp Song, Dong Su Ahn, Seong Gu Kang, Soon Ho Chang, "Influence of the substitution of Fe for Mn on the electrochemical properties of LiMn_2O_4 ", *Solid State Ionics*, Vol. 111, pp. 237–242, 1998.
- [3] Masaki Okada, Yun-Sung Lee, Masaki Yoshio, "cycle characterizations of $\text{LiM}_x\text{Mn}_{2-x}\text{O}_4$ ($\text{M}=\text{Co}, \text{Ni}$) materials for lithium secondary battery at wide voltage region", *J. of Power Sources*, Vol. 90, pp. 196–200, 2000.
- [4] Xiangming He, Jianjun Li, Yan Cai, Yaowu Wang, Jierong Ying, Changyin Jiang, Chunrong Wan, "Fluorine doping of spherical spinel LiMn_2O_4 ", *Solid State Ionics*, Vol. 176, pp. 2571–2576, 2005.
- [5] Katharine R. Stroukoff and Arumugam Manthiram, "Thermal stability of spinel $\text{Li}_{1.1}\text{Mn}_{1.9-y}\text{M}_y\text{O}_{4-z}\text{F}_z$ ($\text{M} = \text{Ni}, \text{Al}$, and Li , $0 \leq y \leq 0.3$, and $0 \leq z \leq 0.2$) cathodes for lithium ion batteries", *J. Mater. Chem.*, Vol. 21, pp. 10165–10170, 2011.
- [6] Q. Luo, T. Muraliganth, A. Manthiram, "On the incorporation of fluorine into the manganese spinel cathode lattice", *Solid State Ionics*, Vol. 180, pp. 703–707, 2009.
- [7] Chuan Wu, Feng Wu, Liquan Chen, Xuejie Huang, "Fabrications and electrochemical properties of fluorine-modified spinel LiMn_2O_4 for lithium ion batteries", *Solid State Ionics*, Vol. 152–153, pp. 327–334, 2002.
- [8] Woo-seong Kim, Kwang-il Chung, young-Kook Choi, Yung-Eun Sung, "Synthesis and charge-discharge properties of $\text{LiNi}_{1-x-y}\text{Co}_x\text{M}_y\text{O}_2$ ($\text{M}=\text{Al}, \text{Ga}$) compounds", *J. power sources*, Vol. 115, pp. 101–109, 2003.
- [9] Gx Wang, S. Bewlay, M. Lindsay, Z.P. Guo, J. Yao, K. Konstantinov, H.K. Liu and S.X. Dou, "Energy Storage materials for Lithium-ion batteries", *Materials Forum* Vol. 27, pp. 33–44, 2004.

- [10] Junlan Xie, Xiang Huang, Zhibin Zhu, Jinhui Dai, "Hydrothermal synthesis of orthorhombic LiMnO_2 nanoparticles", *Ceramics International*, Vol. 37, pp. 419–421, 2011.
- [11] R Thirunakaran, B Ramesh Babu, N Kalaiselvi, P Periasamy, T Prem Kumar, N G Renganathan, M Raghavan and N Muniyandi; "Electrochemical behavior of $\text{LiMyMn}_{2-y}\text{O}_4$ ($M = \text{Cu, Cr; } 0 \leq y \leq 0.4$)", *Bull. Mater. Sci.* vol. 24, pp.51- 55, 2001.
- [12] Hyuu-Soo Kim, Ke-Tack Kim, and Padikkasu Periasamy; *electronic Materials Letters*, "Synthesis and Electrochemical Performances of $\text{LiNi}_{(0.4)}\text{Mn}_{(0.4)}\text{Co}_{(0.2)}\text{O}_2$ Cathode Material for Lithium Rechargeable Battery", Vol. 2 No. 2, pp. 119-126, 2006.
- [13] Leah A. Riley, Sky Van Atta, Andrew S. Cavanagh, Yanfa Yan, Steven M. George, Ping Liuc, Anne C. Dillonb, Se-Hee Lee, "Electrochemical effects of ALD surface modification on combustion synthesized $\text{LiNi}_{1/3}\text{Mn}_{1/3}\text{Co}_{1/3}\text{O}_2$ as a layered-cathode material", *J. of Power Sources*, Vol. 196, pp. 3317–3324, 2011.
- [14] Yassine Bentaleba, Ismael Saadoune, Kenza Mahera, Latifa Saadib, Kenjiro Fujimoto, Shigeru Ito, "On the $\text{LiNi}_{0.2}\text{Mn}_{0.2}\text{Co}_{0.6}\text{O}_2$ positive electrode material", *J. of Power Sources*, Vol. 195, pp. 1510–1515, 2010.
- [15] J.S. Gnanaraj, V.G. Pol, A. Gedanken, D. Aurbach, "Improving the high-temperature performance of LiMn_2O_4 spinel electrodes by coating the active mass with MgO via a sonochemical method", *Electrochemistry Communications* Vol. 5, pp. 940–945, 2003.
- [16] Xianglan Wu, Seung Bin Kim, "Improvement of electrochemical properties of $\text{LiNi}_{0.5}\text{Mn}_{1.5}\text{O}_4$ spinel", *J. of Power Sources*, Vol. 109, pp.53-57, 2002.
- [17] Chen Zhao-yong, Zhu Hua-li, Hu Guo-rong, Xiao Jin, Peng Zhong-dong, Liu Ye-xiang, "Electrochemical performance and structure characteristics of $\text{LiMn}_2\text{O}_{4-x}\text{Y}_x$ ($Y = \text{F, Cl, Br}$) compounds", Vol. 14, pp. 1151-1155, 2004.
- [18] Priti Singh, Anjan Sil, Mala Nath, Subrata Ray, "Synthesis and characterization of $\text{Li}[\text{Mn}_{2-x}\text{Mg}_x]\text{O}_4$ ($x = 0.0-0.3$) prepared by sol-gel synthesis", *Ceramics-Silikaty*, Vol. 54, pp. 38-46, 2010.
- [19] P Periasamy, B Ramesh, H Babu, R Thirunakaran, N Kalaiselvi, T Prem Kumar, N G Renganathan, M Raghavan and N Muniyandi, "Solid-state synthesis and characterization of LiCoO_2 and $\text{LiNi}_y\text{Co}_{1-y}\text{O}_2$ solid solutions", *Bull. Mater. Sci.*, Vol. 23, No. 5, pp. 345–348, 2000.
- [20] Kochoy Fung, Judith C. Chow and John G. Watson "Evaluation of OC/EC Speciation by Thermal Manganese Dioxide Oxidation and the IMPROVE Method", *J. Air & Waste Manage. Assoc.*, Vol. 52, pp. 1333-1341, 2002.